Evolution of genes involved in the unusual genitals of the bear macaque, *Macaca arctoides*

Abstract

Genital divergence is thought to contribute to reproductive barriers by establishing a "lock-and-key" mechanism for reproductive compatibility. One such example, *Macaca arctoides*, the bear macaque, has compensatory changes in both male and female genital morphology as compared to close relatives. *Macaca arctoides* also has a complex evolutionary history, having extensive introgression between the *fascicularis* and *sinica* macaque species groups. Here, phylogenetic relationships were analyzed via whole genome sequences from five species, including *M. arctoides*, and two species each from the putative parental species groups. This analysis revealed ~3x more genomic regions supported placement in the *sinica* species group as compared to the *fascicularis* species group. Additionally, introgression analysis of the *M. arctoides* genome revealed it is a mosaic of recent polymorphisms shared with both species groups. To examine the evolution of their unique genital morphology further, the prevalence of candidate genes involved in genital morphology were compared against genome-wide outliers in various population genetic metrics, while accounting for background variation in recombination rate. This analysis identified 66 outlier genes, including several genes that influence baculum morphology in mice, which were of interest since the bear macaque has the longest primate baculum. The mean of several metrics was statistically different in the candidate genes as compared to the rest of the genome, suggesting that genes involved in genital morphology have increased divergence and decreased diversity beyond expectations. These results highlight how extensive introgression may have contributed to reproductive isolation and shaped the unique genital morphology in the bear macaque.

Keywords: reproductive isolation, hybridization, speciation, baculum

Introduction

In species with internal fertilization, genital morphology may have complex and rapid evolution. This has been extensively demonstrated in males (Eberhard, 1993; Klaczko *et al.*, 2015; Langerhans *et al.*, 2016) and females (Greenway *et al.*, 2019; Simmons & Fitzpatrick, 2019; Sloan & Simmons, 2019). There have been multiple proposed explanations for this including: (1) species isolation via a "lock-and-key" mechanism, (2) sexual conflict, and (3) cryptic female choice (Eberhard, 1985; Sloan & Simmons, 2019). The first explanation suggests that male and female genitalia uniquely coevolve to prevent heterospecific mating. It has historically been dismissed as a general explanation for genital evolution but acknowledged to play a role in particular cases (Eberhard, 1985, 2010). One reason for this dismissal is a presumed lack of variability in female genitalia between species, which suggests the "lock" (female genitalia) is rarely a unique match for the "key" (male genitalia) (Eberhard, 1985; Sloan & Simmons, 2019). However, studies in beetles (Sota & Kubota, 1998), flies (Kamimura & Mitsumoto, 2012), and damselflies (Barnard *et al.*, 2017) have demonstrated reproductive incompatibility between closely related species caused by mechanical mismatch in heterospecific crosses, suggestive of a "lock-and-key" mechanism (Sloan and Simmons, 2019). Sexual conflict may entail either conflict between males trying to obtain mates or conflict between males and females in levels of investment in offspring (Eberhard, 1985). Cryptic female choice happens when male reproductive output may be affected by the female after copulation (Eberhard, 1985, 1996). These processes both involve competition that may also result in species-specific genitalia. For example, a prediction of cryptic female choice is that female genitalia may evolve more rapidly than male genitalia. This can result in compensatory coevolution of male genitalia that causes reproductive isolation between species (Langerhans *et al.*, 2016; Greenway *et al.*, 2019; Sloan & Simmons, 2019). In support of this it has been found that male and female genitalia coevolve in internal fertilizing poecilid fishes (Greenway *et al.*, 2019) and in dung beetles female genitalia diverge more quickly than male genitalia (Simmons & Fitzpatrick, 2019).

Additionally, it has been found that females in populations of dung flies exhibiting sexual conflict have greater preference for conspecific males than females in monogamous populations (Martin & Hosken, 2003).

The bear macaque, *Macaca arctoides*, is unique amongst macaques (and primates generally) for its genital morphology, with distinctive genital characteristics in both sexes (Figure 1). In males, it has the longest baculum of all primates (4-6 cm; Fooden, 1990), even when corrected for body weight (Dixson, 1987; Fooden, 1990). In addition to its elongation, the urethral opening is located on the ventral side of the penis, altering the overall morphology relative to other macaque species (Fooden, 1990). In females, *M. arctoides* female genitalia appear uniquely coadapted to their male counterparts in both length and morphology (Fooden, 1967). Given these compensatory changes, it has been hypothesized that genital evolution in this species followed a "lock-and-key" mechanism, which is likely to be rare amongst primates (Dixson, 1998).

Beyond genital morphology, the mating behavior of the bear macaque has been highlighted in the literature as being atypical amongst macaques. In most other macaques, males and females mount multiply, but perhaps due to the altered male genital morphology, bear macaques engage in a single-mount ejaculatory mating strategy with a prolonged sitting where the males deposit an ejaculatory plug in females (Fooden, 1990). However, most studies have excluded species from the *sinica* species group, except *M. arctoides* (Dixson, 1987; Dixson & Anderson, 2004). In studies looking at *M. radiata,* another member of the *sinica* species group, they also favor a single mount mating style differing from *M. fascicularis* and *M. mulatta* (Shively *et al.*, 1982). Similarly, to *M. arctoides, M. radiata* also exhibits a post-ejaculatory sit. Since both species have larger bacula than species in the *fascicularis* group, the hypothesis that increased baculum aide in prolonged intromission is supported. Therefore, the novelty of mating behavior in the bear macaque may be based on studies that did not include the behavior of representatives from its closest relatives.

73 Additional distinguishing characteristics not related to genital morphology include whitish
74 pelage in newborns, and a bald forehead and cheeks (the latter evident in Figure 2A) (Fooden,
75 1990). Further, the evolutionary history of this species has been noted as extremely complex with
76 early molecular work revealing phylogenetic incongruence between mitochondrial and Y-
77 chromosomal genealogies for *M. arctoides* (Tosi *et al.*, 2000, 2003). Mitochondrial markers place
78 *M. arctoides* as sister to the *fascicularis* species group (includes *M. cyclopis*, *M. fascicularis*,
79 *M. fuscata*, and *M. mulatta*), whereas autosomal markers place it as sister to the *sinica* species group
80 (includes *M. assamensis*, *M. radiata*, *M. sinica*, and *M. thibetana*) (Li *et al.*, 2009b; Jiang *et al.*, 2016; Li
81 *et al.*, 2018; Fan *et al.*, 2018). Similarly, both morphological and Y-chromosomal trees support
82 placement in the *sinica* group (Tosi *et al.*, 2000; Jiang *et al.*, 2016; Fan *et al.*, 2018) (see Table S1 in
83 Fan *et al.*, 2018 for review). This phylogenetic incongruence was hypothesized to be consistent with
84 ancient hybridization between the ancestor of the *fascicularis* species group and a *sinica* species
85 group member (an ancestor of either *M. assamensis* or *M. thibetana*) contributing to hybrid
86 speciation of *M. arctoides* (Tosi *et al.*, 2003).
87 In contrast to allopolyploid speciation, homoploid hybrid speciation (HHS) conserves
88 chromosome number and is postulated to occur with similar frequencies in plants and animals
89 (Mallet, 2007; Mavárez & Linares, 2008). Though expected to be a rare speciation mechanism
90 relative to bifurcating speciation, diverse taxa such as birds (*Passer italiae*; (Elgvin *et al.*, 2017)),
91 sunflowers (Helianthus anomalus; (Rieseberg, 2003)) and yeast (*Saccharomyces paradoxus*;
92 (Leducq *et al.*, 2016)) are thought to have evolved via HHS. Recent analysis of macaque genomes
93 support introgression between *M. arctoides* and members of the *fascicularis* and *sinica* species
94 groups (Fan *et al.*, 2018), both of whom it overlaps with geographically (Figure 2B). These species
95 groups are estimated to have split ~3 million years ago. Recent mitochondrial phylogenetics have
96 shown that *M. arctoides* is more closely related to *M. mulatta* as compared to *M. fascicularis* (Fan *et*
97 *al.*, 2018; Roos *et al.*, 2019), indicating introgression may have occurred after the split of these two

species, which is estimated to be 1.68 mya (Stevison & Kohn, 2009; Jiang *et al.*, 2016; Fan *et al.*, 2018). This timing overlaps glacial periods of the Pleistocene which is associated with reduced expanse of Southeast Asian forests into multiple refugia. Ecological isolation is a common feature to other scenarios of HHS (Gompert *et al.*, 2006). In the case of *M. arctoides*, isolation is hypothesized to have contributed to the extensive interspecific hybridization forcing interbreeding of species that otherwise might have had alternative options for mating (Tosi *et al.*, 2003). Available evidence suggests that this interbreeding subsided ~1.5 mya (Fooden, 1990; Tosi *et al.*, 2003). This hypothesized hybrid origin is diagrammed in Figure S1A, with a range of possible split times indicated by the thick purple line. Regardless of whether the bear macaque is indeed a hybrid species, the evidence for historical hybridization suggests that the dramatic, derived genital morphology may have been influenced by, or evolved despite extensive genetic exchange with other macaque species (Tosi *et al.*, 2000, 2003).

Here, we investigated the potential role of hybridization in shaping the unusual genital morphology of *M. arctoides*. We hypothesized that if the unique genital morphology contributes to reproductive isolation, then genes involved in genital morphology would show extreme population genetic signatures for *M. arctoides*. To test this hypothesis, we compiled a list of 2,284 candidate genes associated with genital morphology in other organisms, with a specific focus on mammals. We used an existing recombination rate map for *M. mulatta* to identify outliers in several population genetic metrics, such as introgression, nucleotide diversity, and divergence. Phylogenomic and population genetic approaches were used on several extant macaque species (*M. arctoides;* the *sinica* group species *M. thibetana* and *M. assamensis*; and the *fascicularis* group species *M. fascicularis* and *M. mulatta*). We found 66 of the candidate genes were significant genome outliers in at least one of seven population genetic metrics. Further, the mean across 4/7 population genetic metrics was significantly different in the candidate genes as compared to all other genes in the genome. Interestingly, three dN/dS outliers were associated with putative

123 baculum morphology in mice. Overall, our results suggest that genital evolution in the bear
124 macaque has been extensive and involved a large number of genes associated with various
125 phenotypic changes in both males and females.

126 **Methods**

127 ***Samples and Genome Sequencing***

128 One female each from *M. arctoides* (Malaya) and *M. assamensis* (A20) were sequenced. The
129 *M. arctoides* sample was from the Malaka Zoo in Malaysia (previously described in Tosi *et al.*, 2000).
130 Due to their now vulnerable conservation status, and restricted international trade, availability of
131 these species is severely restricted, severely limiting sample sizes (see Discussion). These two
132 samples were multiplexed and sequenced on one lane of sequencing for initial quality assessment.
133 They were then subsequently run on one additional lane of sequencing each for a final 1.5 lanes per
134 sample. Sequencing was done at UCSF Medical Center Sequencing Facility on an Illumina HiSeq
135 2000 machine. Each run was assigned as different read groups to be treated as independent in the
136 variant calling workflow. The raw read data have been deposited in the NCBI sequence read archive
137 and are available via the accession PRJNA622565 (see Table 1).

138 ***Publicly available sequences***

139 Raw FASTQ files were downloaded from 8 public genome samples for this project (Table 1).
140 Genome samples were selected to be representative of the taxa relevant for *M. arctoides* evolution.
141 For the *fascicularis* group, many more public sequences were available than used here, however we
142 selected two sequencing projects and included all samples from both projects, including those with
143 lower coverage (<10X, see Table 1). This sample size was chosen to allow for equal representation
144 across the various species groups. Additional sample details can be found in the corresponding
145 publications (Yan *et al.*, 2011; Fan *et al.*, 2014, 2018). These were downloaded from NCBI SRA using
146 sratoolkit version 2.8.1 with options to split data into read pairs and in the original format

147 (*ncbi/sra-tools*, 2008). Because *M. thibetana* was sequenced on an older platform, we used seqtk (Li,
148 2019) to convert from Q64 to Q33. Additionally, SRA files from multiple lanes as indicated in the
149 FASTQ header were split for independent alignment to the reference genome facilitating the
150 definition of separate read groups to be treated as independent in the variant calling workflow.

151 ***Alignment, genome analysis, and variant calling***

152 Raw FASTQ files from all samples were aligned to the reference genome rheMac8 (NCBI
153 Accession: PRJNA214746). The masked reference genome was downloaded from UCSC. The
154 reference genome for rheMac8 includes 20 autosomes, a pair of sex chromosomes, a mitochondrial
155 genome, and 284,705 unnamed scaffolds of varying length. The total length of all scaffolds is 3.2Gb.
156 The total length of all named chromosomes is 2.8 Gb. GATK best practices were followed to obtain
157 high quality variant sites (see Supplementary Methods and Tables S1-S2). Briefly, reads were
158 aligned to the reference genome, duplicates were marked, indels were realigned, base quality
159 scores were recalibrated, variants were called, and variant quality scores were recalibrated.
160 Samples from each species were processed independently and merged into a final callset (see Data
161 Availability). The baboon reference genome was added to the variant files via two-way genome
162 alignment and custom scripts that are available via GitHub. These final filtered files for each
163 chromosome with the baboon information are freely available and were used for all subsequent
164 analyses. A more detailed workflow is described in both the supplement as well as the GitHub page
165 for the project, which includes command prompts and custom scripts (see Data Availability).

166 ***Four-taxon test for introgression***

167 To analyze patterns of introgression in sliding windows, a modified four-taxon test was
168 used (Figure S2). Rather than separately analyzing gene flow between *M. arctoides* and each
169 parental species group, as has been done previously (Fan *et al.*, 2018), we relied on the modified
170 statistic f_{dM} (Malinsky *et al.*, 2015), which is suggested to perform better than other related statistics

171 based on simulation results (Martin *et al.*, 2015). Specifically, hybridization between the three
172 samples of *M. arctoides* (P3) was tested with samples from the *sinica* species group (P1) and the
173 *fascicularis* species group (P2), using the baboon reference genome as an outgroup (papAnu4; see
174 Supplement for details). Our approach differed from the typical way these tests are setup where
175 one may only be interested in shared ancestry between two pairs of taxa, (P1:P3 and P2:P3), and
176 the P1 and P2 taxa are more closely related to each other than either are to P3 (see Figure 2 in
177 Kulathinal *et al.*, 2009). However, this modification allowed for the quantification of shared
178 ancestry from both putative parents together. It is worth noting that previous work had similar
179 results when using the more traditional four taxon test setup for these taxa (Fan *et al.*, 2018).
180 Calculations of f_{dM} were done using scripts available on GitHub (Martin, 2019) and using
181 several differently sized genomic windows. f_{dM} was computed for overlapping windows of size 5kb,
182 25kb, 50kb, 100kb, 500kb and 1000kb, with a step size of 20% of each window size. The minimum
183 number of sites per window size was based on the distribution of sites available in the callset at
184 each bin size. Specifically, a minimum number of sites of 10, 50, 100, 200, 1000, and 2000,
185 respectively, per window size were used. Because it is recommended to have at least 100 sites per
186 window (Martin, 2019), the 50kb window size was selected and the results are presented in Figure
187 2 as a heatmap across the genome. Results from the additional bin sizes are shown in Figure S3.
188 This analysis was repeated with individual taxa from each species group (Table S3).

189 ***Topology weighting***

190 To analyze the weights of different phylogenetic topologies across the genome, the software
191 Twisst was used to compare the weights of different species topologies throughout the genome
192 (Martin & Belleghem, 2017; Martin *et al.*, 2019). First, data used for the introgression analysis were
193 pruned to make sure that each group had at least one member represented in the genotype data.
194 Next, neighbor joining trees were constructed in sliding windows of 50 SNPs each across the

genome using Phyml from scripts available on GitHub (Martin, 2019). This generated newick formatted tree files that were used as input for Twisst. The resulting weight distributions among the three possible topologies were summed across the genome (Figure 2D).

The topology weighted outputs were further explored by collapsing adjacent intervals with the same majority topology supported. Since there were three possible topologies, the majority topology was defined as any one topology that had at least two-thirds of the total weight values. Any intervals without a majority topology were labeled as "unresolved". If adjacent intervals supported the same majority topology, they were collapsed. The data were subsequently split into the three major topologies. These were intersected with gene regions from the Ensembl annotations for rheMac8 downloaded from UCSC.

Bootstrap confidence intervals for topo1, topo2, topo3, and unresolved proportions were computed by resampling 2,792 1 Mbp intervals along the genome (149 when considering only chromosome X) for each of 10,000 replicates and taking the 2.5% and 97.5% quantiles.

Divergence Analysis

Based on the three possible topologies, nucleotide divergence was calculated as D_{xy} using scripts available on GitHub (Martin, 2019). First, stringency in defining the majority topology was increased to require 100% of the weights be on only one of the three topologies. Next, divergence was calculated between M. ***arctoides and members of the fascicularis species group (M.*** fascicularis and M. mulatta) for regions with regions with topo3 ((arc,fas),sin). ***As well, divergence was calculated between M. arctoides and members of the sinica species group (M. assamensis and M. thibetana) for genomic regions with topo2 (fas,(arc,sin)).*** For the regions with topo1 (arc,(fas,sin)), the relative divergences were unchanged when divergence was calculated between *M. arctoides* and members of the *sinica* species group as compared to divergence calculated

218 between *M. arctoides* and members of the *fascicularis* species group, therefore only the latter is
219 reported.

220 ***Candidate Gene Selection***

221 A major criterion of homoploid hybrid speciation is evidence that RI evolved as a by-
222 product of hybridization (Schumer *et al.*, 2014). This coupled with the unique genital morphology of
223 both males and females in the bear macaque (Figure 1) led us to focus our study on candidate genes
224 that have been identified in other studies to be associated with genital morphology. We conducted a
225 literature search for terms associated with genital morphology such as "disorder of sex
226 development", "DSD", "baubellum", and "baculum", the latter two terms included due to the
227 extremely large baculum of the bear macaque, and the female equivalent structure. We filtered to
228 remove genes that solely associated with either fertility or adult hormonal disorders/shifts as these
229 conditions are unlikely to affect the development of genitalia. Included in our initial list of 141
230 genes (Table S4) were genes associated with gonad dysgenesis (Bamshad *et al.*, 1997; Ekici *et al.*,
231 2013; Witchel, 2018; Lavi *et al.*, 2020), female masculinization (Wang *et al.*, 2020), genital tubercle
232 formation (Haraguchi *et al.*, 2000), baculum morphology (Schultz *et al.*, 2016a), hypogonadism
233 (Délot *et al.*, 2017), gonad differentiation (Witchel, 2018), gonad development (Witchel, 2018), sex
234 determination (Délot *et al.*, 2017), and sex differentiation (Délot *et al.*, 2017).

235 In addition to our literature search, we used the Human Phenotype Ontology (HPO)
236 (Robinson *et al.*, 2008) database to target search terms associated with genital abnormalities,
237 specifically targeting those that would likely be developmental. We therefore targeted the HPO
238 category "Abnormal Reproductive System Morphology", but removing categories that were
239 unrelated, such as "Genital Ulcers". A list of the HPO terms can be found in Table 2. In total, this
240 added 1230 genes to our 141 set of literature candidate genes. It is worth noting that 88 genes
241 overlapped between these lists, with the remainder being unique to our literature search.

242 Additionally, because certain phenotypes are lacking in humans, such as the baculum, we
243 did a similar search of the Mammalian Phenotype (MP) Browser
244 (http://www.informatics.jax.org/vocab/mp_ontology) available through the Mouse Genome
245 Database. We used largely overlapping search terms to the HPO terms, totaling a set of 1554 genes.
246 As expected, there were several genes that overlapped across each set, but also many genes unique
247 to each query. In sum, our final candidate gene list comprised of 2,284 genes from the literature, as
248 well as the HPO and MP databases that had orthologs in the rheMac8 reference genome (Table 2).
249 Of these 2,284 genes, only a subset was used in the calculations of each population genetic metric
250 based on constraints of these subsequent analyses. The major limiting factor was the data for
251 recombination rate, which was used to identify genomic outliers. The total number of genes
252 analyzed for each statistic is reported in Table S6 and summarized in Table 2. For most statistics,
253 1,055 candidate genes were included in the population genetic analysis for outliers.

254 ***Outlier Analysis***

255 With the candidate gene list, we sought to identify if any genes on our list had extreme
256 values for diversity, differentiation, or introgression within the bear macaque. To do this, we took a
257 gene centered approach. Instead of the pre-defined windows used earlier, we used the Ensembl
258 Gene Annotations for rheMac8 to define window coordinates. First, the smallest region containing
259 all transcripts from the annotation file was computed. Then, 5kb upstream and downstream was
260 added to include potential regulatory regions for each gene. These windows were used to re-
261 calculate f_{dM}, and to calculate nucleotide diversity, pi. We also chose to look at two metrics for
262 nucleotide divergence – F_{ST} and D_{XY} – calculated to compare *M. arctoides* to members of the both the
263 *fascicularis* and *sinica* species groups separately. All metrics were calculated using scripts available
264 on GitHub (Martin, 2019). Finally, we estimated dN/dS for each gene. This methodology was
265 previously described in (Bailey & Stevison, 2021). Briefly, we used the three possible gene tree

266 topologies to estimate a branch specific dN/dS for the *M. arctoides* branch for every gene in the
267 genome. Estimates where dS was 0 and dN/dS was greater than 10 were excluded as these genes
268 had insufficient divergence to obtain valid estimates (Villaneuva-Canas et al. 2013). Then, the
269 topology weights for each gene window from our Twisst analysis were used to weight the dN/dS
270 estimates for each gene across the three gene trees.

271 To further identify extreme values of each metric, we took into consideration that many of
272 these statistics have been shown to be correlated with recombination rate, which can impede the
273 detection of outliers, specifically enriching for outliers in regions of low recombination rate
274 (Stevison & McGaugh, 2020). Therefore, we also computed an average recombination rate for each
275 gene. For this, we download the UCSC track for recombination rate associated with rheMac8
276 (ftp://ftp.hgsc.bcm.edu/ucscHub/rhesusSNVs/rheMac8/all.rate.bw) (Xue *et al.*, 2016) and
277 converted it from bigwig to bedGraph format using UCSC utilities. Bedtools (Quinlan & Hall, 2010)
278 was then used to calculate the average recombination rate (cM/Mb) in each gene interval.

279 Finally, the Cook's distance (*cooksd*) (Cook & Weisberg, 1982) was calculated from a linear
280 regression between each statistic and recombination rate per gene. Cook's distance provides a
281 measure of the leverage and residual values of a particular data point, which indicates how much it
282 influences the overall regression. Thus, it reveals how much the regression changes when that
283 observation is removed, making it useful for identifying outliers in a regression analysis. Here,
284 extreme values were determined based on genes that were 3*mean(*cooksd*) above or below the
285 fitted value in the regression model, depending on the particular statistic. The resulting outlier
286 genes were genes where the statistic being evaluated (e.g. F_{ST}, D_{XY}) was much higher/lower than
287 expected when considering the relationship between the statistic and recombination rate. For f_{dM},
288 because it is a two-tailed distribution, outliers from both the upper and lower end of the
289 distribution were computed. For dN/dS, we did not find a statistically significant relationship with
290 recombination rate, consistent with prior findings in humans (Coop & Przeworski, 2007).

291 Therefore, we used a 5% cutoff for extreme values of this statistic instead of the Cook's distance
292 approach. This percentage produced fewer genome-wide outliers than the average of all other
293 metrics, suggesting it as an appropriate cutoff (Table S6).

294 Genes identified as genome-wide outliers were then compared against our set of *a priori*
295 candidate genes to identify outliers that were putatively involved in genital morphology. A chi-
296 square test was conducted to determine if the number of outliers that were in our candidate gene
297 set were more than expected due to random chance. A summary of the regression results and chi-
298 square tests can be found in Table S6, and the resulting **66** outlier genes that overlapped our
299 candidate gene set can be found in Table S7. BCFtools (version 1.11) (Li *et al.*, 2009a) view was
300 used to extract VCFs for the 66 outlier genes and these 66 VCFs were combined and annotated
301 using SnpEff (version 4.3p) (Cingolani *et al.*, 2012) to examine the putative impacts of variants
302 identified within this system. The Mmul_8.0.1.86 annotation was downloaded through SnpEff to
303 conduct this analysis as this corresponds to the reference genome used for samples in this study.
304 These annotations include exons, introns, UTRs and regions 5kb upstream and downstream of start
305 and end sites for genes to account for possible regulatory factors. These annotations are provided
306 in tabular format in Table S7.

307 ***Permutation Analyses***

308 Permutation tests were used to identify differences in various summary statistics (F_{ST}, D_{XY},
309 f_{dM}, dN/dS, and pi) between candidate genital genes and all other genes. For calculations of pi this
310 was a one-tailed test where genital genes were expected to have reduced pi in *M. arctoide*s
311 compared to other genes. For calculations of dN/dS this was a one-tailed test where genital genes
312 were expected to have increased dN/dS in *M. arctoides* compared to other genes. All other
313 comparisons (F_{ST}, D_{XY}, and f_{dM}) were two-tailed tests. In all of these tests the test statistic used was
314 the difference of the mean summary statistic for the candidate genital genes and the mean for the

315 same summary statistic for all other genes. These analyses were conducted using modified perl
316 scripts from Evans et al. (2021) and the results are reported in Table S6.
317 In addition to this, we conducted permutation analyses on genes categorized as being
318 involved in either male or female genital development or abnormalities according to the HPO and
319 MP databases. Specifically, the categories used were HP:0010461, HP:0010460, MP:0009198 and
320 MP:0009208 (see Table S5). This was done to examine the possibility of male and female genital
321 morphology evolving at different rates (see Introduction). These analyses parallel the above in
322 examining the same summary statistics, though all tests were two-tailed as there was not a specific
323 expectation for the direction of evolution.

324 **Results**

325 Genomic analysis of five macaque species revealed a mosaic of evolutionary ancestry with
326 respect to two major species groups. These analyses used newly sequenced whole genome samples
327 from *M. arctoides* (20X coverage) and *M. assamensis* (13X), and 8 publicly available genomes
328 ranging in coverage from 4-49X (median 32X; Table 1). Most variable positions were heterozygous
329 in only one species (Figure 2C). For shared variants, *M. arctoides* shares the most variants with the
330 *sinica* species group, *M. assamensis* and *M. thibetana*, consistent with taxonomic placement in this
331 species group (Fooden, 1980). However, the two-way intersection between *M. arctoides* and *M.*
332 *thibetana* had the fewest shared heterozygous sites, which is likely due to the low overall
333 heterozygosity in the *M. thibetana* sample (Figure 2C; Table 1). *M. assamensis* had the largest
334 number of heterozygous sites (~4.7 million; Table 1; Figure 2C).

335 ***Extensive Mosaicism of the M. arctoides Genome***

336 The four-taxon test (Kulathinal *et al.*, 2009; Green *et al.*, 2010; Martin *et al.*, 2015) results
337 which used all three *M. arctoides* samples, supported that the *M. arctoides* genome has a mosaic of
338 shared ancestry with both the *sinica* and *fascicularis* species groups (Figure 3), which is consistent

339 with extensive introgression from both species groups, though some of these windows with shared
340 ancestry could also be due to incomplete lineage sorting between these taxa (Stevison & Kohn,
341 2009) (See Supplementary Materials). The genome-wide average f_{dM} (Malinsky *et al.*, 2015; Martin,
342 2019) value was -0.113, ranging from -0.69 (with negative values supporting shared ancestry with
343 the *sinica* group) and 0.55 (with positive values supporting shared ancestry with the *fascicularis*
344 group) in 50kb sliding windows. This sliding window analysis was repeated with several window
345 sizes (Figure S3), and all had a similar genome-wide mean f_{dM}. In a previous study, estimates of
346 Patterson's *D* (Green *et al.*, 2010) were similar to the f_{dM} estimates here (see Table S8 in (Fan *et al.*,
347 2018)).

348 Phylogenetic relationships among the species groups were evaluated via the software
349 Twisst (Martin & Belleghem, 2017) (topology weighting by iterative sampling of subtrees). This
350 method quantifies phylogenetic relationships across the genome and returns weights in sliding
351 windows (Figure 2D). The topology weights were used to define a "majority topology" as having
352 two-thirds or more of the sum of weights in any region. Windows that did not meet this criterion
353 were re-classified as "unresolved". This analysis showed the proportion of the genome that
354 supported "topo2" (fas,(arc,sin)), which groups *M. arctoides* with the *sinica* group, as 52.64% (95%
355 bootstrap CI [52.02%, 53.28%]). However, a significant portion, 15.70% (95% bootstrap CI
356 [15.40%, 16.01%]), of the genome supported "topo3" ((arc,fas),sin), which groups *M. arctoides* with
357 the *fascicularis* species group. Interestingly, 11.07% (95% bootstrap CI [10.84%, 11.31%]) of the
358 genome supported *M. arctoides* clustering in a group by itself outside of the *sinica* and *fascicularis*
359 groups ("topo1"; (arc,(fas,sin))). The remaining 20.59% (95% bootstrap CI [20.18%, 21.01%]) of
360 the genome was categorized as unresolved because none of the three topologies had >2/3^{rds} weight.
361 That the 95% confidence intervals of topo3 do not overlap with those of topo1 is consistent with
362 the putative hybrid origin of *M. arctoides*, as opposed to topo1 and topo3 both stemming from
363 ancestral polymorphism.

364 However, a subsequent investigation of nucleotide divergence of these genomic regions
365 revealed that D_{XY} between sister taxa in regions supporting topo2 (fas,(arc,sin)) were significantly
366 lower than regions supporting topo3 ((arc,fas),sin) (Figure S5). This result is consistent with either
367 *M. arctoides* being sister to the *fascicularis* group with subsequent hybridization with the *sinica*
368 species group (Figure S1B), or that *M. arctoides* split from macaques prior to the split of the *sinica*
369 and *fascicularis* species groups with subsequent hybridization from each group at different times
370 (Figure S1C). This latter scenario is consistent with the deepest nucleotide divergence being in
371 regions supporting topo1 (arc(sin,fas)). However, it is worth pointing out that this analysis does not
372 include additional members of the *sinica* species group (e.g. *M. sinica* and *M. radiata*) that would be
373 crucial to resolving this complex evolutionary history (see Supplementary Materials).

374 ***Investigation of outlier genes associated with genital morphology***

375 Our gene centered approach led to the calculation of seven major population genetic
376 statistics across all genes in the rheMac8 annotation. In total, our analysis focused primarily on
377 10,543 genes for which we were able to get reliable estimates for each metric, including
378 recombination rate (Table S6). However, for the dN/dS calculations, this baseline number of genes
379 was far fewer with only 1903 due to the limitation of our approach (see Methods). Of the 2,284
380 genes that were included on our candidate gene list (Table 2 and S4) and also had orthologs in
381 rheMac8, only 1,055 were included in our most analyses (Table 2 and S6). Of the genome-wide
382 outliers across these metrics, 66 of these 1,055 genes were statistically elevated as potential
383 outliers for further investigation (Table S7).

384 A chi-square test was used to compare the proportion of outlier candidate genes (OCGs)
385 against those analyzed to the expected number of outliers based on the remainder of the genes in
386 the genome (Table S6). This analysis revealed that there were no more outliers than expected by
387 chance, suggesting that the 66 outliers is not more than would be expected of any other set of

388 candidate genes. However, a permutation test was used to compare the difference between means
389 across the seven population genetic metrics found that for four metrics, the mean of the candidate
390 genes was significantly different than expected based on the value across the remainder of the
391 genes in the genome (Figure 4). These metrics showed that the nucleotide diversity, pi, across the
392 candidate genes was significantly lower than expected (Figure 4A). Additionally, both measures of
393 F_{ST} between *M. arctoides* and the two species groups revealed higher than expected nucleotide
394 divergence (Figure 4C-D). Similarly, D_{XY} between *M. arctoides* and the *fascicularis* species group was
395 much higher than expected based on 100 permutations of a similar number of genes that were not
396 part of the candidate gene set.

397 An investigation into the 66 genes found that three genes were OCGs across four statistics
398 (CEP19, GATA3, and PTPN23). Three more genes were OCGs across three statistics (AIRE, CSPP1,
399 and SNAI2). Finally, 11 genes were OCGs across two of the seven statistics (CAMKV, DND1, HMGA1,
400 HSPA4, KDM3B, PIK3CA, PSMB8, SIN3A, TDRKH, TMED10, and ZCWPW1). It is worth noting that
401 although the genes on the HPO and MP database lists were under the specific search terms, each of
402 these genes were associated with many unrelated phenotypes, thus it is difficult to interpret their
403 overall significance in this analysis. For OCGs from the HPO database, each gene had an average of
404 70 phenotypic terms with a range from 4 to 302. For the OCGs in the mammalian phenotype
405 database, the average number of phenotypic terms was smaller at 22.6, and the range was from 1 to
406 96. This suggests the mammalian database may be slightly better curated to avoid genes that are
407 overly pleiotropic. Interestingly, of these 17 OCGs that were outliers across more than one statistic,
408 only two have putative high impact variants (CEP19 and CSPP1), with the latter also having 15
409 missense mutations of putative moderate impact. CSPP1 is associated with 151 HPO terms, being
410 presumably involved in a lot of different phenotypes (Table S7).

411 Despite the uncertainty of hits in the larger databases, seven of the OCGs were on the
412 original literature survey for candidate genes (Table 2 and S4), which were more carefully selected

413 based on their role in genital morphology. Of these, GATA3 was an outlier across multiple statistics,
414 which was initially included due to its known associated with urogenital anomalies (Délot *et al.*,
415 2017), with over 20 years of research on this gene (Lemos & Thakker, 2020), including knockout
416 studies (Grote *et al.*, 2008). Another of these seven is HFE, which is associated with hereditary
417 hemochromatosis (HH) and subsequent hypogonadism (Délot *et al.*, 2017) due to decreased iron
418 circulation (Bezwoda *et al.*, 1977; McDermott & Walsh, 2005), with symptoms such as decreased
419 libido and testicular atrophy in humans (Kelly *et al.*, 1984). In our SNP effect analysis, GATA3 had 1
420 predicted moderate impact variant and 8 low impact variants (Table S7).
421 Additionally, two of the seven OCGs from the literature survey gene list were CYP proteins
422 (CYP17A1 and CYP21A2). Both CYP17A1 and CYP21A2 are associated with congenital adrenal
423 hyperplasia (CAH aka 17OHD), a disorder which leads to abnormal sexual development (Délot *et al.*,
424 2017), with CYP21A2 mutations being the most common cause of CAH (Koppens *et al.*, 1992).
425 CYP21A2 mutations in humans have been associated with simple virilization, in which female
426 genitalia are masculinized during development (Koppens *et al.*, 1992). Several cohort studies have
427 found genotype-to-phenotype associations linking CYP21A2 mutations to a variety of CAH
428 phenotypes (Torres *et al.*, 2003; Soardi *et al.*, 2008; de Carvalho *et al.*, 2016). Additionally, protein
429 structure analysis has been done to examine the impact of specific mutants on a form of CAH known
430 as salt-water wasting disease, which if left undiagnosed leads to low sodium levels and death
431 (Haider *et al.*, 2013). CYP17A1 is heavily involved in steroidogenesis, with deletion mutations
432 leading to hormone production inhibition and sex development abnormalities (Keskin *et al.*, 2015;
433 Turkkahraman *et al.*, 2015; Zhang *et al.*, 2015; Papi *et al.*, 2018; Xia *et al.*, 2021). Recent genome
434 studies of 17OHD patients revealed 46,XY karyotype in physically presenting females which co-
435 occur with multiple mutations in the CYP17A1 gene (Zhang *et al.*, 2015; Xia *et al.*, 2021). CYP21A1
436 had two high, 21 moderate, and 32 low impact variants, whereas CYP17A1 had two moderate and

437 eleven low impact variants (Table S7). Additionally, CYP21A1 had the highest proportion of silent
438 and nonsense variants, as well as the 2nd highest proportion of missense variants (Figure 5).
439 Three more OCGs on the original literature candidate gene list that were outliers for dN/dS
440 were identified in a study as major candidates for baculum morphology in mice (Schultz *et al.*,
441 2016a) (DACT1, PTPRC, and ASPM; Figure 4). This is particularly intriguing when one considers the
442 unique baculum morphology of the *os penis* in the bear macaque relative to all other primates (see
443 Discussion). Because these were outliers for dN/dS, which is targeted to the protein coding regions
444 of the gene, we further investigated the protein sequence of each gene to look at coding mutations.
445 PTPRC had the highest proportion of missense mutation among the seven literature outliers (Figure
446 5). Specifically, there were seven amino acid changes in multiple individuals, two of which
447 overlapped the fibronectin domain and had significant changes in the amino acid properties. Two of
448 these changes were completely fixed in *M. arctoides* (p.K449E and p.R424R), two were nearly fixed,
449 shared only with a single *M. assamensis* sample (p.E314G and p.Y359S), and three amino acid
450 changes were shared between *M. arctoides* and members of the *fascicularis* species group (p.D363G,
451 p.K384N, and p.D385N). DACT1 had the 2nd highest proportion of silent variants among the seven
452 literature OCGs (Figure 5). Additionally, we found 3 major amino acid changes clustered together,
453 two that were nearly fixed in *M. arctoides* as compared to all other macaques (p.C439Y and
454 p.G493D). Additionally, there was a p.Q498R mutation that was shared between *M. arctoides* and
455 members of the *fascicularis* species group. This similarity is of particular interest due to the shared
456 baculum morphology of these species (see Discussion). Finally, for ASPM, there was only one fixed
457 amino acid change (p.H352P), which overlapped a region of the protein that interacts with another
458 enzyme called katanin. Additionally, there was a p.H1870R mutation that was shared with *sinica*
459 species, and several other amino acid changes that were unique to *M. arctoides*, but polymorphic
460 rather than fixed (p.V269F, p.T357I, and p.R1164H). While all of these amino acid changes are likely
461 to have an impact on the protein, the specific changes to the gene function and its overall

462 implications for the baculum phenotype are unknown. Still, these residues would be of particular
463 interest in mouse mutant studies on the genetics of baculum morphology.
464 Permutation analysis of male versus female genital development genes showed no
465 significant difference in all statistics except f_{dM} (p = 0.02), where male genital genes exhibited higher
466 introgression between *M. arctoides* and *sinica* species than female genes (Table S5).

467 **Discussion**

468 ***Genital morphology genes have higher divergence and lower diversity than expected***

469 Although the number of outliers from our genital candidate genes was not more than
470 expected by chance, the average divergence was higher than expected and the diversity was lower
471 than expected (Figure 4). In fact, none of the permutations overlapped the observed mean
472 difference between the actual candidate gene set for four of the seven population genetic metrics.
473 Specifically, the candidate genes had lower nucleotide diversity (pi) which is consistent with recent
474 positive selection on these genes that would have reduced local genetic variation. Similarly, F_{ST}
475 between *M. arctoides* and both species groups was higher than expected, which is also consistent
476 with positive selection on this subset of genes as compared to the remainder of the genome.
477 Additionally, D_{XY} between *M. arctoide*s and *fascicularis* species was elevated, but not D_{XY} between
478 *M. arctoides* and *sinica* species. These results suggest that the evolution of these genes have been
479 increased relative to the rest of the genes in the genome, confirming the importance of genital
480 morphology in the evolution of this species. A possible explanation for the difference in the two
481 measures of nucleotide divergence is that F_{ST} is a relative measure of divergence, whereas D_{XY} is an
482 absolute measure (Noor & Bennett, 2009). Here, the majority of the genome clusters with *sinica*
483 species, which could explain why D_{XY} between *M. arctoide*s and the *sinica* species group does not
484 have more outliers than expected.

485 Of 66 candidate genes identified as outliers, many are involved in a variety of phenotypes.
486 Of course, because these are developmental phenotypes, it is not surprising that the impact of these
487 genes would be highly pleiotropic. However, their specific role in contributing to the divergent
488 genital morphology and subsequent reproductive isolation in this species is unclear. One
489 interesting thing worth noting is that the number of genes in both phenotype onotology databases
490 associated with male genital abnormalities is nearly 2x the number of genes associated with female
491 genital abnormalities (Table 2). This is not likely due to underlying differences in the genetics of
492 these traits, but instead more likely reflects a bias towards research into male reproductive
493 morphology as compared to female reproductive abnormalities. Still, for the most part, the mean
494 values across our various metrics were not significantly different between these sets of male vs.
495 female genes (Table S5). While the result for f_{dM} was statistically significant, both values were lower
496 than the genome-wide mean, and thus do not likely reflect differences in the direction of
497 introgression. In contrast, the difference in means of dN/dS, though not statistically significant, had
498 twice the difference of f_{dM}. Specifically, the mean dN/dS across male genes (0.141) matches the
499 mean of the genome background (0.143), whereas the mean across female genes was much lower
500 (0.101). Though speculative, this difference is perhaps consistent with the idea that many genes of
501 large effect on female genital morphology have yet to be described, supported by the disparity in
502 the gene set sizes. Together these findings suggests that future work should aim to identify
503 additional potentially undiscovered genes that play a role in female genital morphology.

504 ***Divergent baculum morphology putatively explained by dN/dS outliers***

505 Regardless of the inconclusiveness of the genes that were found based on phenotype
506 ontology methods, 3/21 outliers for dN/dS were genes previously identified in mice as candidate
507 genes for morphological variation in the baculum (DACT1, PTPRC, and ASPM). The baculum, or
508 penis bone, is a novel male genital structure in placental mammals that evolved ~145 million years

509 ago (Brindle & Opie, 2016), with the bear macaque, having the longest primate baculum. Since that
510 time, it has been gained or lost multiple times, including recent loss in Homo sapiens (Schultz et al.,
511 2016b; Carosi & Scalici, 2017). Despite its remarkable interspecific variation, the penis bone
512 generally does not vary extensively within species (Ramm et al., 2009), and may be the only
513 physical trait that differs consistently between closely related species, making it a key
514 morphological character for species identification (Carosi & Scalici, 2017). However, the genetics of
515 morphological variation in this trait are only beginning to be understood. In 2016, a morphometric
516 analysis using micro-CT scans of bacula in mice identified three major quantitative trait loci (QTLs),
517 two that together explained 50.6% of the variation in baculum size, and one that explained 23.4%
518 of the variation in baculum shape (Schultz *et al.*, 2016a). These regions were further narrowed by
519 both differential gene expression in early development of male mice, and potential involvement in
520 bone or genital morphogenesis, revealing 16 major candidate loci with potential effects on baculum
521 development and morphology (see Table S3 in (Schultz *et al.*, 2016a)), that were included on our
522 candidate gene list (Table S4).

523 The baculum in *M. arctoides* is more than double the average length of *sinica* species group
524 taxa and nearly four times as long as *fascicularis* species group taxa (Fooden, 1971; Dixson, 1987).
525 In addition to its elongation, the morphology of the *M. arctoides* baculum also has a unique arced
526 crescent shape, with an absent distal region that is present in most other macaque species (See
527 comparison in Figure 8 of Fooden *et al.*, 1985; Fooden, 1990). Among macaques, these two features
528 – a gentle dorsoventral curvature and the lack of a well-defined distal process – are shared only by
529 members of the *fascicularis* species group. This latter point perhaps explains why 4/5 amino acid
530 changes across these three genes that were shared between *M. arctoides* and another group, were
531 shared between *M. arctoides* and the *fascicularis* species members. This is in stark contrast to the
532 rest of the genome which has a much higher proportion of shared variation with *sinica* species
533 group members.

534 ***Future Directions***

535 This study has focused on genes with phenotypic associations with genital morphology, but
536 an outlier analysis can only present hypotheses of the specific genes involved in the divergent
537 reproductive traits of the bear macaque. Therefore, the 66 outlier genes are candidates that may
538 have contributed to speciation. The target of future functional work should be to identify their
539 specific role (if any) in contributing to either divergent male genital morphology or compensatory
540 changes in female reproductive morphology. They should also be the target of functional studies in
541 model systems, such as mice, on genital morphology of both males and females. For example, the
542 seven fixed amino acid changes in the bear macaque across the three dN/dS outlier genes
543 associated with mouse baculum morphology should be prioritized in future work on the genetics of
544 this trait. Still, why this remarkable trait is divergent in the bear macaque is unknown. Perhaps
545 more detailed functional connections between specific genes/variants and the baculum would
546 allow for future work to examine the selective processes that shaped this unique genital phenotype.
547 Additionally, as the genetic basis of other genital traits, such as baubellum morphology
548 become known, the candidate gene list can be extended. Similarly, as the genome annotation
549 improves with subsequent reference genomes, more genes can be considered that have clear
550 orthologs in macaques.
551 In addition to this study, there has been extensive interest in the evolution of this species.
552 However, due to the limited number of publicly available whole genome samples (now three with
553 the present study), the conservation status of this species, and the ethical and logistical barriers to
554 experimental research with primates, it is challenging to make functional insights into its evolution.
555 Additional WGS data from more individuals of this species would allow for a better characterization
556 of selection/adaptation within this lineage. Additionally, more WGS samples would be useful in
557 examining the distribution of introgression haplotype lengths to pinpoint the timing of events in
558 this system that would better clarify when hybridization from each parent took place.

559
560 **References**

561 Bailey, N.P. & Stevison, L.S. 2021. Mitonuclear conflict in a macaque species exhibiting
562 phylogenomic discordance. *Journal of Evolutionary Biology* **34**: 1568–1579.

563 Bamshad, M., Lin, R.C., Law, D.J., Watkins, W.S., Krakowiak, P.A., Moore, M.E., *et al.* 1997. Mutations
564 in human TBX3 alter limb, apocrine and genital development in ulnar-mammary syndrome.
565 *Nat Genet* **16**: 311–315.

566 Barnard, A.A., Fincke, O.M., McPeek, M.A. & Masly, J.P. 2017. Mechanical and tactile incompatibilities
567 cause reproductive isolation between two young damselfly species: MATING STRUCTURES
568 AND REPRODUCTIVE ISOLATION. *Evolution* **71**: 2410–2427.

569 Bezwoda, W.R., Bothwell, T.H., Van Der Walt, L.A., Kronheim, S. & Pimstone†, B.L. 1977. An
570 Investigation into Gonadal Dysfunction in Patients with Idiopathic Haemochromatosis.
571 *Clinical Endocrinology* **6**: 377–385.

572 Brindle, M. & Opie, C. 2016. Postcopulatory sexual selection influences baculum evolution in
573 primates and carnivores. *Proceedings of the Royal Society B: Biological Sciences* **283**:
574 20161736. Royal Society.

575 Carosi, M. & Scalici, M. 2017. Baculum (Os Penis). In: *The International Encyclopedia of Primatology*,
576 pp. 1–5. American Cancer Society.

577 Cingolani, P., Platts, A., Wang, L.L., Coon, M., Nguyen, T., Wang, L., *et al.* 2012. A program for
578 annotating and predicting the effects of single nucleotide polymorphisms, SnpEff: SNPs in
579 the genome of Drosophila melanogaster strain w ^{1118}; iso-2; iso-3. *Fly* **6**: 80–92.

580 Conway, J. & Gehlenborg, N. 2019. *UpSetR: A More Scalable Alternative to Venn and Euler Diagrams*
581 *for Visualizing Intersecting Sets*. CRAN, https://CRAN.R-project.org/package=UpSetR.

582 Cook, R.D. & Weisberg, S. 1982. *Residuals and Influence in Regression*. New York: Chapman and Hall.

583 Coop, G. & Przeworski, M. 2007. An evolutionary view of human recombination. *Nat. Rev. Genet.* **8**:
584 23–34.

585 Danecek, P., Auton, A., Abecasis, G., Albers, C.A., Banks, E., DePristo, M.A., *et al.* 2011. The variant call
586 format and VCFtools. *Bioinformatics* **27**: 2156–8.

587 de Carvalho, D.F., Miranda, M.C., Gomes, L.G., Madureira, G., Marcondes, J.A.M., Billerbeck, A.E.C., *et*
588 *al.* 2016. Molecular CYP21A2 diagnosis in 480 Brazilian patients with congenital adrenal
589 hyperplasia before newborn screening introduction. *Eur J Endocrinol* **175**: 107–116.

590 Délot, E.C., Papp, J.C., DSD-TRN Genetics Workgroup, Sandberg, D.E. & Vilain, E. 2017. Genetics of
591 Disorders of Sex Development: The DSD-TRN Experience. *Endocrinol Metab Clin North Am*
592 **46**: 519–537.

593 Dixson, A.F. 1987. Observations on the evolution of the genitalia and copulatory behaviour in male
594 primates. *Journal of Zoology* **213**: 423–443.

595 Dixson, A.F. 1998. *Primate sexuality: comparative studies of the prosimians, monkeys, apes, and*
596 *human beings*. Oxford University Press, Oxford; New York.

597 Dixson, A.F. & Anderson, M.J. 2004. Sexual behavior, reproductive physiology and sperm
598 competition in male mammals. *Physiology & Behavior* **83**: 361–371.

599 Eberhard, W.G. 1993. Evaluating Models of Sexual Selection: Genitalia as a Test Case. *The American*
600 *Naturalist* **142**: 564–571. The University of Chicago Press.

601 Eberhard, W.G. 2010. Evolution of genitalia: theories, evidence, and new directions. *Genetica* **138**:
602 5–18.

603 Eberhard, W.G. 1996. *Female control: sexual selection by cryptic female choice*. Princeton University
604 Press, Princeton, N.J.

605 Eberhard, W.G. 1985. *Sexual selection and animal genitalia*. Harvard University Press, Cambridge,
606 Mass.

607 Ekici, A.B., Strissel, P.L., Oppelt, P.G., Renner, S.P., Brucker, S., Beckmann, M.W., *et al.* 2013. HOXA10
608 and HOXA13 sequence variations in human female genital malformations including
609 congenital absence of the uterus and vagina. *Gene* **518**: 267–272.

610 Elgvin, T.O., Trier, C.N., Tørresen, O.K., Hagen, I.J., Lien, S., Nederbragt, A.J., *et al.* 2017. The genomic
611 mosaicism of hybrid speciation. *Science Advances* **3**: e1602996.

612 Evans, B.J., Peter, B.M., Melnick, D.J., Andayani, N., Supriatna, J., Zhu, J., *et al.* 2021. Mitonuclear
613 interactions and introgression genomics of macaque monkeys (*Macaca*) highlight the
614 influence of behaviour on genome evolution. *Proc. R. Soc. B.* **288**: 20211756.

615 Fan, Z., Zhao, G., Li, P., Osada, N., Xing, J., Yi, Y., *et al.* 2014. Whole-Genome Sequencing of Tibetan
616 Macaque (Macaca thibetana) Provides New Insight into the Macaque Evolutionary History.
617 *Mol Biol Evol* **31**: 1475–1489.

618 Fan, Z., Zhou, A., Osada, N., Yu, J., Jiang, J., Li, P., *et al.* 2018. Ancient hybridization and admixture in
619 macaques (genus Macaca) inferred from whole genome sequences. *Molecular Phylogenetics*
620 *and Evolution* **127**: 376–386.

621 Fooden, J. 1980. Classification and Distribution of Living Macaques (Macaca Lacepede, 1799). In:
622 *The Macaques: Studies in Ecology, Behavior, and Evolution* (D. G. Lindburg, ed), pp. 1–9. Van
623 Nostrand Reinhold Company, New York.

624 Fooden, J. 1967. Complementary Specialization of Male and Female Reproductive Structures in the
625 Bear Macaque, Macaca arctoides. *Nature* **214**: 939–941. Nature Publishing Group.

626 Fooden, J. 1971. Male external genitalia and systematic relationships of the Japanese macaque
627 (Macaca fuscata Blyth, 1875). *Primates* **12**: 305–311.

628 Fooden, J. 1990. The bear macaque,Macaca arctoides: a systematic review. *Journal of Human*
629 *Evolution* **19**: 607–686.

630 Fooden, J., Guoqiang, Q., Zongren, W. & Yingxiang, W. 1985. The stumptail macaques of China.
631 *American Journal of Primatology* **8**: 11–30.

632 Gompert, Z., Fordyce, J.A., Forister, M.L., Shapiro, A.M. & Nice, C.C. 2006. Homoploid Hybrid
633 Speciation in an Extreme Habitat. *Science* **314**: 1923–1925.

634 Green, R.E., Krause, J., Briggs, A.W., Maricic, T., Stenzel, U., Kircher, M., *et al.* 2010. A draft sequence
635 of the Neandertal genome. *Science* **328**: 710–722.

636 Greenway, R., McNemee, R., Okamoto, A., Plath, M., Arias-Rodriguez, L. & Tobler, M. 2019. Correlated
637 divergence of female and male genitalia in replicated lineages with ongoing ecological
638 speciation. *Evolution* **73**: 1200–1212.

639 Grote, D., Boualia, S.K., Souabni, A., Merkel, C., Chi, X., Costantini, F., *et al.* 2008. Gata3 Acts
640 Downstream of β-Catenin Signaling to Prevent Ectopic Metanephric Kidney Induction. *PLOS*
641 *Genetics* **4**: e1000316. Public Library of Science.

642 Haider, S., Islam, B., D'Atri, V., Sgobba, M., Poojari, C., Sun, L., *et al.* 2013. Structure–phenotype
643 correlations of human CYP21A2 mutations in congenital adrenal hyperplasia. *PNAS* **110**:
644 2605–2610. National Academy of Sciences.

645 Haraguchi, R., Suzuki, K., Murakami, R., Sakai, M., Kamikawa, M., Kengaku, M., *et al.* 2000. Molecular
646 analysis of external genitalia formation: the role of fibroblast growth factor (Fgf) genes
647 during genital tubercle formation. *Development* **127**: 2471–2479.

648 Jiang, J., Yu, J., Li, J., Li, P., Fan, Z., Niu, L., *et al.* 2016. Mitochondrial Genome and Nuclear Markers
649 Provide New Insight into the Evolutionary History of Macaques. *PLoS One* **11**.

650 Kamimura, Y. & Mitsumoto, H. 2012. Lock-and-key structural isolation between sibling Drosophila
651 species: Genital lock-and-key in Drosophila. *Entomological Science* **15**: 197–201.

652 Kelly, T.M., Edwards, C.Q., Meikle, A.W. & Kushner, J.P. 1984. Hypogonadism in Hemochromatosis:
653 Reversal with Iron Depletion. *Ann Intern Med* **101**: 629–632. American College of
654 Physicians.

655 Keskin, M., Uğurlu, A.K., Savaş-Erdeve, Ş., Sağsak, E., Akyüz, S.G., Çetinkaya, S., *et al.* 2015. 17α-
656 Hydroylase/17,20-lyase deficiency related to P.Y27*(c.81C>A) mutation in CYP17A1 gene. *J*
657 *Pediatr Endocrinol Metab* **28**: 919–921.

658 Klaczko, J., Ingram, T. & Losos, J. 2015. Genitals evolve faster than other traits in Anolis lizards.
659 *Journal of Zoology* **295**: 44–48.

660 Koppens, P.F., Hoogenboezem, T., Halley, D.J., Barendse, C.A., Oostenbrink, A.J. & Degenhart, H.J.
661 1992. Family studies of the steroid 21-hydroxylase and complement C4 genes define 11
662 haplotypes in classical congenital adrenal hyperplasia in The Netherlands. *Eur J Pediatr*
663 **151**: 885–892.

664 Kulathinal, R.J., Stevison, L.S. & Noor, M.A.F. 2009. The Genomics of Speciation in Drosophila:
665 Diversity, Divergence, and Introgression Estimated Using Low-Coverage Genome
666 Sequencing. *PLoS Genet* **5**.

667 Langerhans, R.B., Anderson, C.M. & Heinen-Kay, J.L. 2016. Causes and Consequences of Genital
668 Evolution. *Integr Comp Biol* **56**: 741–751. Oxford Academic.

669 Lavi, E., Zighan, M., Abu Libdeh, A., Klopstock, T., Weinberg-Shukron, A., Renbaum, P., *et al.* 2020. A
670 Unique Presentation of XY Gonadal Dysgenesis in Frasier Syndrome due to WT1 Mutation
671 and a Literature Review. *Pediatr Endocrinol Rev* **17**: 302–307.

672 Leducq, J.-B., Nielly-Thibault, L., Charron, G., Eberlein, C., Verta, J.-P., Samani, P., *et al.* 2016.
673 Speciation driven by hybridization and chromosomal plasticity in a wild yeast. *Nature*
674 *Microbiology* **1**: 15003.

675 Lemos, M.C. & Thakker, R.V. 2020. Hypoparathyroidism, deafness, and renal dysplasia syndrome:
676 20 Years after the identification of the first GATA3 mutations. *Human Mutation* **41**: 1341–
677 1350.

678 Li, H. 2019. *Toolkit for processing sequences in FASTA/Q formats: lh3/seqtk*. Github,
679 https://github.com/lh3/seqtk.

680 Li, H., Handsaker, B., Wysoker, A., Fennell, T., Ruan, J., Homer, N., *et al.* 2009a. The Sequence
681 Alignment/Map format and SAMtools. *Bioinformatics* **25**: 2078–2079.

682 Li, J., Fan, Z., Sun, T., Peng, C., Yue, B. & Li, J. 2018. Comparative Genome-Wide Survey of Single
683 Nucleotide Variation Uncovers the Genetic Diversity and Potential Biomedical Applications
684 among Six Macaca Species. *Int J Mol Sci* **19**.

685 Li, J., Han, K., Xing, J., Kim, H.-S., Rogers, J., Ryder, O.A., *et al.* 2009b. Phylogeny of the macaques
686 (Cercopithecidae: Macaca) based on Alu elements. *Gene* **448**: 242–249.

687 Malinsky, M., Challis, R.J., Tyers, A.M., Schiffels, S., Terai, Y., Ngatunga, B.P., *et al.* 2015. Genomic
688 islands of speciation separate cichlid ecomorphs in an East African crater lake. *Science* **350**:
689 1493–1498.

690 Mallet, J. 2007. Hybrid speciation. *Nature* **446**: 279–283.

691 Martin, O.Y. & Hosken, D.J. 2003. The evolution of reproductive isolation through sexual conflict.
692 *Nature* **423**: 979–982.

693 Martin, S. 2019. *General tools for genomic analyses.* Github,
694 https://github.com/simonhmartin/genomics_general.

695 Martin, S.H. & Belleghem, S.M.V. 2017. Exploring Evolutionary Relationships Across the Genome
696 Using Topology Weighting. *Genetics* **206**: 429–438.

697 Martin, S.H., Davey, J.W. & Jiggins, C.D. 2015. Evaluating the Use of ABBA–BABA Statistics to Locate
698 Introgressed Loci. *Mol Biol Evol* **32**: 244–257.

699 Martin, S.H., Davey, J.W., Salazar, C. & Jiggins, C.D. 2019. Recombination rate variation shapes
700 barriers to introgression across butterfly genomes. *PLOS Biology* **17**: e2006288.

701 Mavárez, J. & Linares, M. 2008. Homoploid hybrid speciation in animals. *Molecular Ecology* **17**:
702 4181–4185.

703 McDermott, J.H. & Walsh, C.H. 2005. Hypogonadism in Hereditary Hemochromatosis. *The Journal of*
704 *Clinical Endocrinology & Metabolism* **90**: 2451–2455.

705 *ncbi/sra-tools*. 2008. NCBI - National Center for Biotechnology Information/NLM/NIH.

706 Noor, M.A.F. & Bennett, S.M. 2009. Islands of speciation or mirages in the desert? Examining the role
707 of restricted recombination in maintaining species. *Heredity* **103**: 439–444.

708 Papi, G., Paragliola, R.M., Concolino, P., Di Donato, C., Pontecorvi, A. & Corsello, S.M. 2018. 46,XY
709 Disorder of Sex Development Caused by 17α-Hydroxylase/17,20-Lyase Deficiency due to
710 Homozygous Mutation of CYP17A1 Gene: Consequences of Late Diagnosis. *Case Rep*
711 *Endocrinol* **2018**: 2086861.

712 Quinlan, A.R. & Hall, I.M. 2010. BEDTools: a flexible suite of utilities for comparing genomic features.
713 *Bioinformatics* **26**: 841–2.

714 Ramm, S.A., Khoo, L. & Stockley, P. 2009. Sexual selection and the rodent baculum: an intraspecific
715 study in the house mouse (Mus musculus domesticus). *Genetica* **138**: 129.

716 Rieseberg, L.H. 2003. Major Ecological Transitions in Wild Sunflowers Facilitated by Hybridization.
717 *Science* **301**: 1211–1216.

718 Robinson, P.N., Köhler, S., Bauer, S., Seelow, D., Horn, D. & Mundlos, S. 2008. The Human Phenotype
719 Ontology: a tool for annotating and analyzing human hereditary disease. *Am J Hum Genet*
720 **83**: 610–615.

721 Roos, C., Kothe, M., Alba, D.M., Delson, E. & Zinner, D. 2019. The radiation of macaques out of Africa:
722 Evidence from mitogenome divergence times and the fossil record. *Journal of Human*
723 *Evolution* **133**: 114–132.

724 Schultz, N.G., Ingels, J., Hillhouse, A., Wardwell, K., Chang, P.L., Cheverud, J.M., *et al.* 2016a. The
725 Genetic Basis of Baculum Size and Shape Variation in Mice. *G3 (Bethesda)* **6**: 1141–1151.

726 Schultz, N.G., Lough-Stevens, M., Abreu, E., Orr, T. & Dean, M.D. 2016b. The Baculum was Gained and
727 Lost Multiple Times during Mammalian Evolution. *Integr Comp Biol* **56**: 644–656.

728 Schumer, M., Rosenthal, G.G. & Andolfatto, P. 2014. How Common Is Homoploid Hybrid Speciation?
729 *Evolution* **68**: 1553–1560.

730 Shively, C., Clarke, S., King, N., Schapiro, S. & Mitchell, G. 1982. Patterns of sexual behavior in male
731 macaques. *American Journal of Primatology* **2**: 373–384.

732 Simmons, L.W. & Fitzpatrick, J.L. 2019. Female genitalia can evolve more rapidly and divergently
733 than male genitalia. *Nat Commun* **10**: 1312.

734 Sloan, N.S. & Simmons, L.W. 2019. The evolution of female genitalia. *J Evol Biol* **32**: 882–899.

735 Soardi, F.C., Barbaro, M., Lau, I.F., Lemos-Marini, S.H.V., Baptista, M.T.M., Guerra-Junior, G., *et al.*
736 2008. Inhibition of CYP21A2 Enzyme Activity Caused by Novel Missense Mutations
737 Identified in Brazilian and Scandinavian Patients. *The Journal of Clinical Endocrinology &*
738 *Metabolism* **93**: 2416–2420.

739 Sota, T. & Kubota, K. 1998. Genital Lock-and-Key as a Selective Agent against Hybridization.
740 *Evolution* **52**: 1507–1513.

741 Stevison, L.S. & Kohn, M.H. 2009. Divergence population genetic analysis of hybridization between
742 rhesus and cynomolgus macaques. *Mol. Ecol.* **18**: 2457–2475.

743 Stevison, L.S. & McGaugh, S.E. 2020. It's time to stop sweeping recombination rate under the
744 genome scan rug. *Molecular ecology*.

745 Torres, N., Mello, M.P., Germano, C.M.R., Elias, L.L.K., Moreira, A.C. & Castro, M. 2003. Phenotype and
746 genotype correlation of the microconversion from the CYP21A1P to the CYP21A2 gene in
747 congenital adrenal hyperplasia. *Braz J Med Biol Res* **36**: 1311–1318. Associação Brasileira de
748 Divulgação Científica.

749 Tosi, A.J., Morales, J.C. & Melnick, D.J. 2000. Comparison of Y Chromosome and mtDNA Phylogenies
750 Leads to Unique Inferences of Macaque Evolutionary History. *Molecular Phylogenetics and*
751 *Evolution* **17**: 133–144.

752 Tosi, A.J., Morales, J.C. & Melnick, D.J. 2003. Paternal, Maternal, and Biparental Molecular Markers
753 Provide Unique Windows Onto the Evolutionary History of Macaque Monkeys. *Evolution* **57**:
754 1419–1435.

755 Turkkahraman, D., Guran, T., Ivison, H., Griffin, A., Vijzelaar, R. & Krone, N. 2015. Identification of a
756 Novel Large CYP17A1 Deletion by MLPA Analysis in a Family with Classic 17α-Hydroxylase
757 Deficiency. *SXD* **9**: 91–97. Karger Publishers.

758 Waal, F.B.M. de. 2004. Peace Lessons from an Unlikely Source. *PLOS Biology* **2**: e101. Public Library
759 of Science.

760 Wang, S., Lawless, J. & Zheng, Z. 2020. Prenatal low-dose methyltestosterone, but not
761 dihydrotestosterone, treatment induces penile formation in female mice and guinea pigs†.
762 *Biology of Reproduction* **102**: 1248–1260.

763 Witchel, S.F. 2018. DISORDERS OF SEX DEVELOPMENT. *Best Pract Res Clin Obstet Gynaecol* **48**: 90–
764 102.

765 Xia, J., Liu, F., Wu, J., Xia, Y., Zhao, Z., Zhao, Y., *et al.* 2021. Clinical and Genetic Characteristics of 17 α-
766 Hydroxylase/17, 20-Lyase Deficiency: c.985_987delTACinsAA Mutation of CYP17A1
767 Prevalent in the Chinese Han Population. *Endocrine Practice* **27**: 137–145. Elsevier.

768 Xue, C., Raveendran, M., Harris, R.A., Fawcett, G.L., Liu, X., White, S., *et al.* 2016. The population
769 genomics of rhesus macaques (Macaca mulatta) based on whole-genome sequences.
770 *Genome Res.* **26**: 1651–1662.

771 Yan, G., Zhang, G., Fang, X., Zhang, Y., Li, C., Ling, F., *et al.* 2011. Genome sequencing and comparison
772 of two nonhuman primate animal models, the cynomolgus and Chinese rhesus macaques.
773 *Nature Biotechnology* **29**: 1019–1023.

774 Zhang, M., Sun, S., Liu, Y., Zhang, H., Jiao, Y., Wang, W., *et al.* 2015. New, recurrent, and prevalent
775 mutations: Clinical and molecular characterization of 26 Chinese patients with 17alpha-

776 hydroxylase/17,20-lyase deficiency. *The Journal of Steroid Biochemistry and Molecular*
777 *Biology* **150**: 11–16.

778

Figures

Figure 1. Diverged genital morphology in male and female bear macaques. *M. arctoides* has divergent male and female genital morphology (top), relative to *M. mulatta* (bottom) representing mechanical isolation between these species. *M. mulatta* morphology is representative of other species in macaques. Male external genitalia for each species are shown on the left (from Fig 3 of Dixson, 1987) and female reproductive tracts are shown on the right (from Fig 4 of Fooden, 1967). Reproduced with permission. Divergent traits for male genitalia include size and shape. Divergent traits for female reproductive tracts include depth of the uterine cavity, width of the vagina, opening size, and urethra location. Scales on the left are in 1 cm divisions.

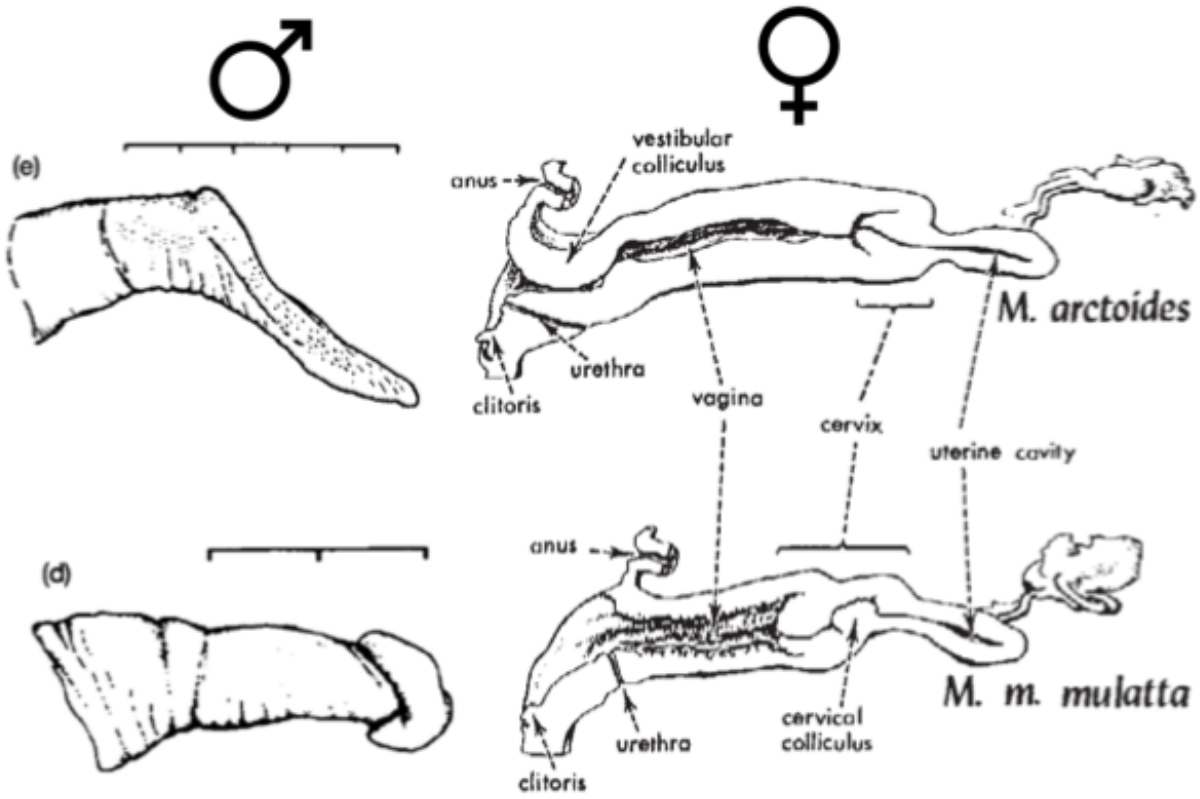

Figure 2. Summary of focal species, *Macaca arctoides*, its evolutionary relationships, and the data used. (a) *M. arctoides* has unique genital morphology and is a putative homoploid hybrid species. Image "Stumptail Monkeys" from (Waal, 2004) by Frans de Waal licensed under CC. (B) Geographic range of *M. arctoides* and other focal species in this study. *M. arctoides* has present day geographic overlap with members of both species groups (redrawn from (Fooden, 1980)). Background image "Topographic map of East Asia" by Ksiom is licensed under CC BY-SA 3.0. This study included WGS from *M. arctoides* and representative members of each species group (Table 1). Baboon was used as an outgroup species. (C) Intersection of heterozygous sites between the five species. The output of vcf-compare from vcftools (Danecek *et al.*, 2011) was input into the UpSetR package (Conway & Gehlenborg, 2019) to plot the intersection of sites. Values in the left plot match count of heterozygous sites per sample in Table 1. (D) Topology weight distribution of three rooted topologies of species relationships in sliding windows along the genome. bab - *P. anubis*.

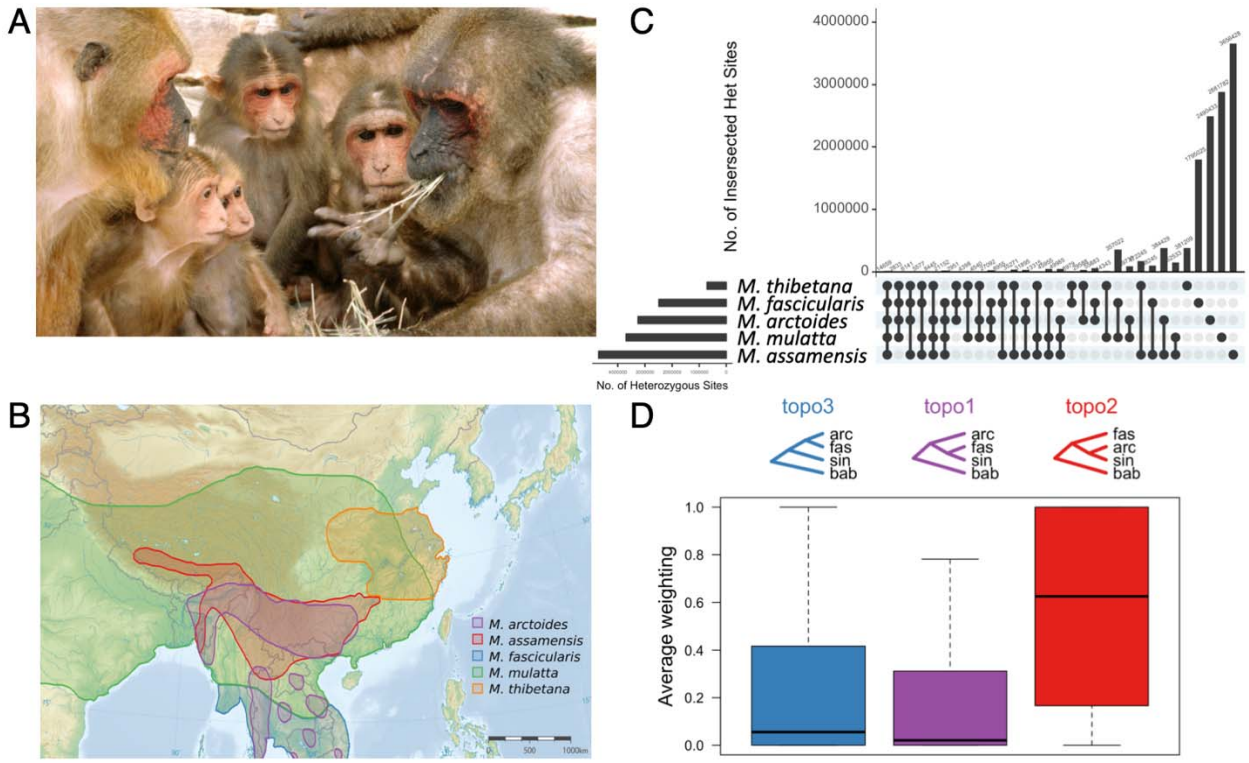

Figure 3. Introgression analysis. Results from analysis of introgression (f_{dM}) between *M. arctoides* samples and the parent taxa in 50kb sliding windows. Regions where *M. arctoides* has most recent ancestry with the *sinica* group are displayed as negative values and regions where *M. arctoides* shares most recent common ancestry with the *fascicularis* group are displayed as positive values. Other window size results are in Figure S3 and plots using individual *M. arctoides* samples are in Figure S4.

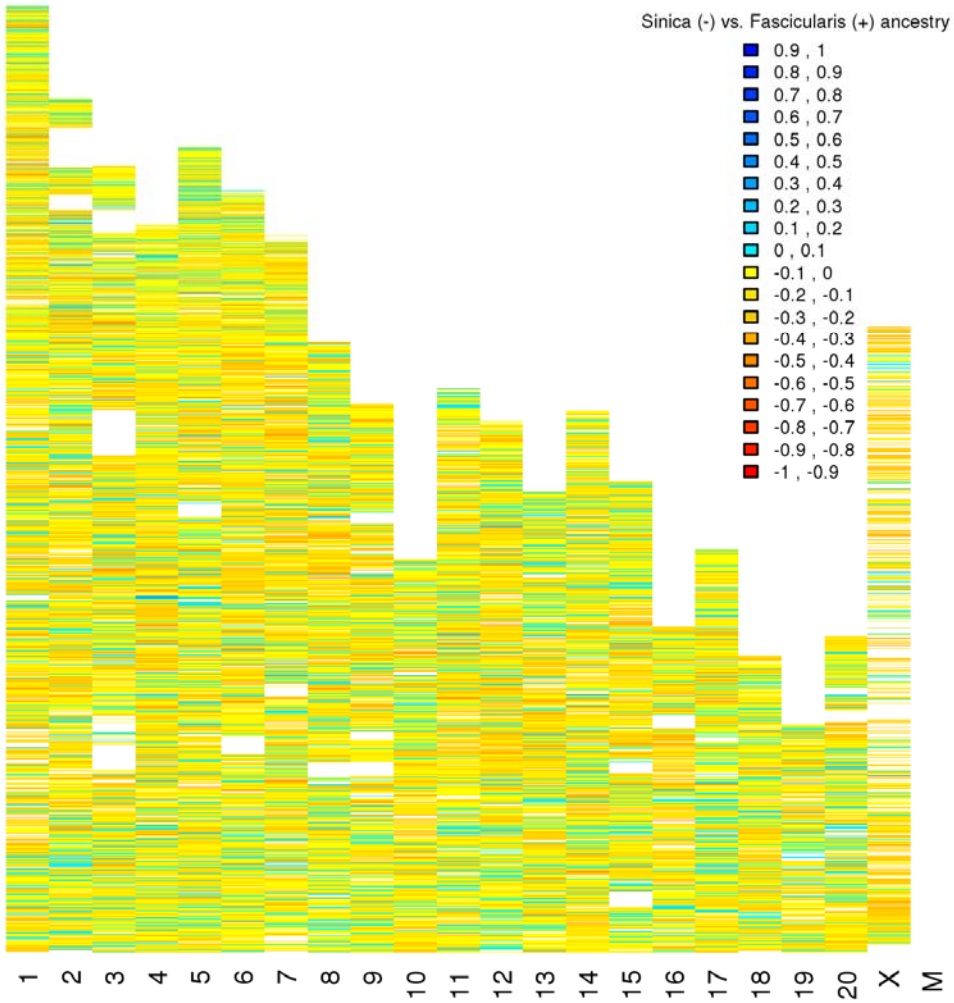

Figure 4. Permutation test results. For each panel, the red line is the difference of the mean of genital genes and all other genes for a given summary statistic. Additionally, a histogram of the results from 100 permutations where the mean difference was recalculated using the same number of randomly selected genes as the candidate genital genes is shown. The various summary statistics plotted here are A) pi in *M. arctoides*, B) D_{XY} between *M. arctoides* and *fascicularis* group species, C) F_{ST} between *M. arctoides* and *fascicularis* group species, and D) F_{ST} between *M. arctoides* and *sinica* group species. The computed p-values for all tests shown here were zero. The remaining statistics were not significantly different and are reported in Table S6 and Figure SX.

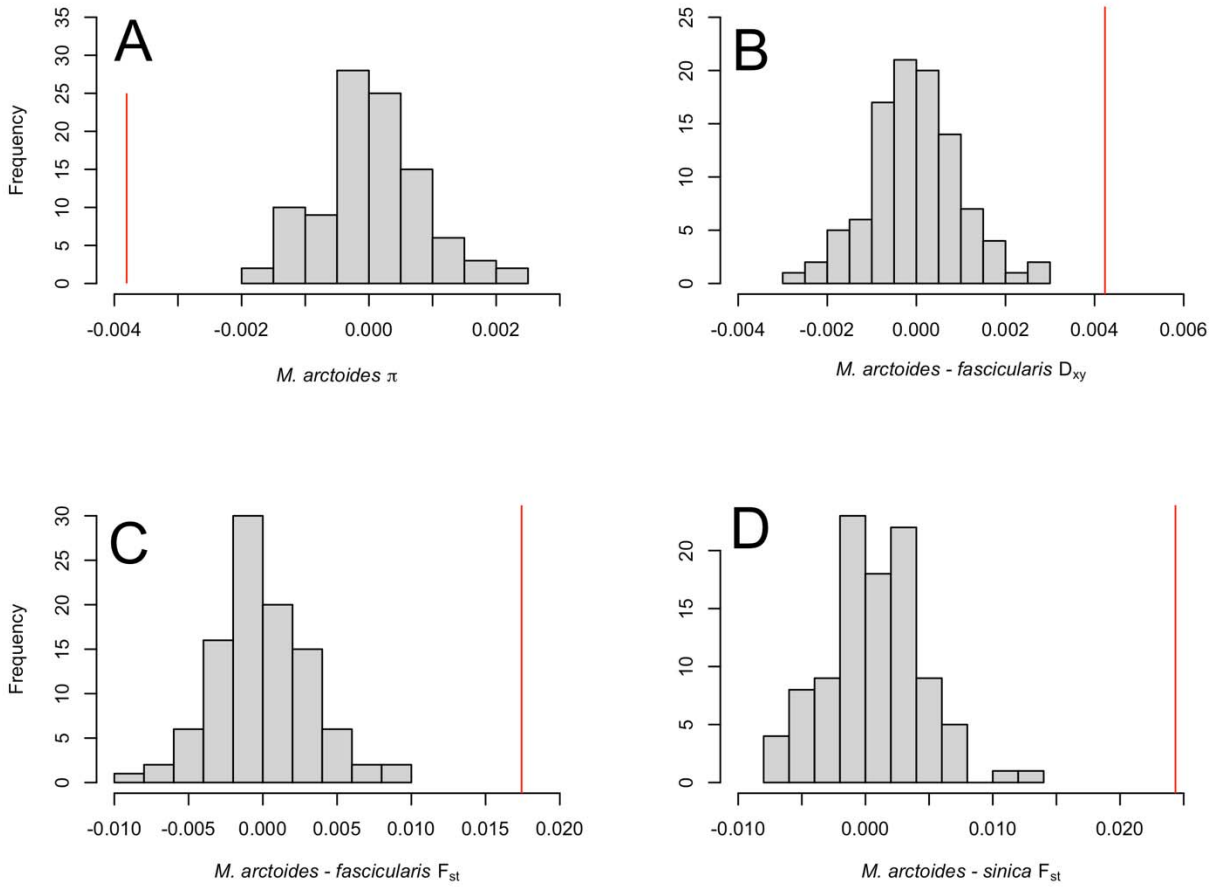

822 **Figure 5. Functional Impact of Variants in Outlier Candidate Genes.** Results from SNPeff are
823 shown broken down by functional impact to the protein sequence of the seven outlier candidate
824 genes based on the literature list. Functional classes are missense variants which change the amino
825 acid, nonsense, which result in a premature stop codon, and silent variants, which alter the
826 nucleotide sequence, but result in a synonymous amino acid.

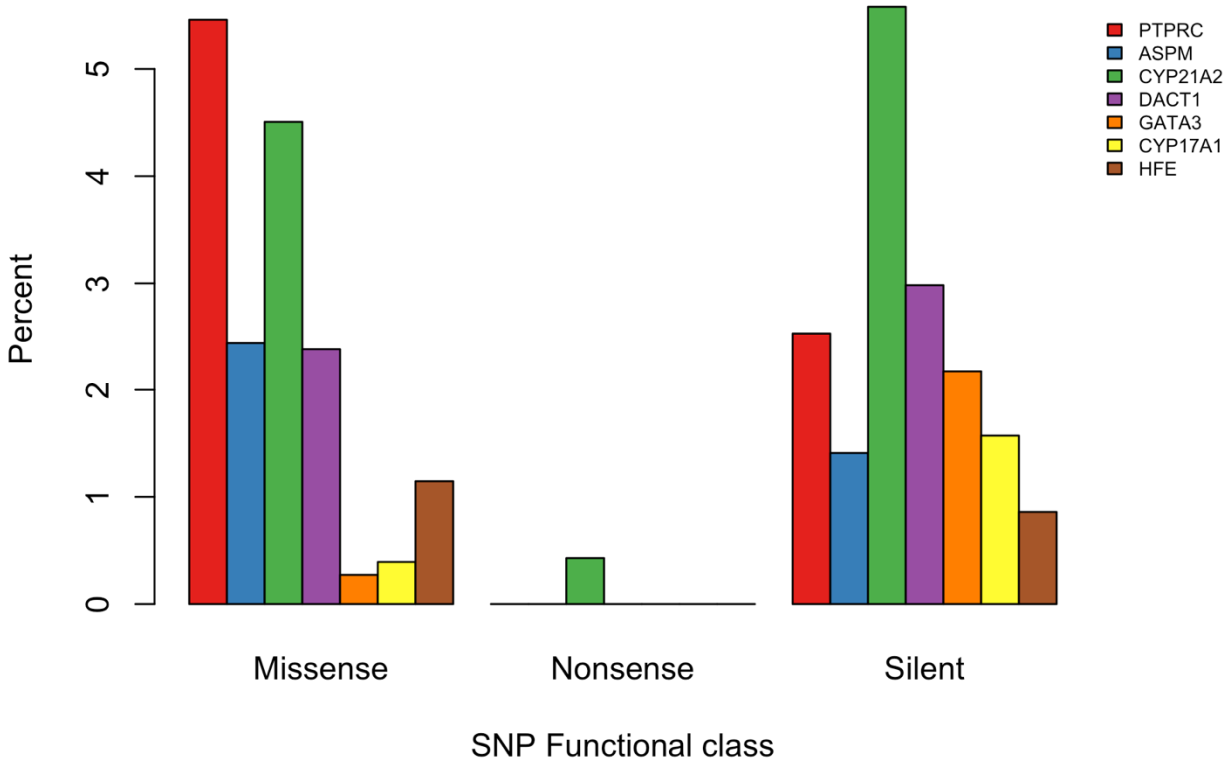

827
828

Tables

Table 1. Sample information. A list of samples used in this study with a summary of genome information. Two samples were sequenced as part of this study (in bold) and the remainder were downloaded from NCBI.

ID	species	Species Group	Coverage	No. sites VQSR Passed	No. sites heterozygous	NCBI Accession	SAMN_ID	Sex
Malaya	***M. arctoides***	**arctoides**	**20**	**6,849,957**	**3,252,204**	**SRS6488501**	**14521207**	**F**
SM1	*M. arctoides*	arctoides	32	6,848,826	3,251,892	SRR2981139	04316319	F
SM2	*M. arctoides*	arctoides	19	6,833,185	3,246,931	SRR2981140	04316320	F
BGI-CE-4	*M. fascicularis*	fascicularis	43	4,547,767	2,486,762	SRS114988	00116341	F
CR-5	*M. mulatta*	fascicularis	44	4,561,581	3,693,024	SRS115022	00113489	F
BGI	*M. mulatta*	fascicularis	10	4,531,187	3,678,452	SRS212016	00627571	M
BGI-96346	*M. mulatta*	fascicularis	4	4,334,465	3,533,580	SRS114988	00113455	M
A20	***M. assamensis***	**sinica**	**13**	**7,567,951**	**4,680,934**	**SRS6491954**	**14521608**	**F**
XH1	*M. assamensis*	sinica	49	7,669,854	4,702,055	SRR2981114	04316321	M
Tibetan-macaque-NO.3	*M. thibetana*	sinica	27	4,844,002	713,449	SRR1024051	02390221	F

Table 2. Summary of candidate gene lists. In addition to a manually curated list from the literature, several phenotype terms were mined from the Human Phenotype Onotology (HPO) and the Mammalian Phenotype (MP) Databases. Here the number of genes associated with each term is listed along with the number of orthologs in rheMac8. Further, the number of genes used in our analysis where we calculated seven population genetics metrics are listed along with the final number of outliers per candidate gene set.

Unique ID	Subontology	Database	# of Genes	# rheMac8 orthologs	# genes analyzed dN/dS	# genes analyzed other stats	# outliers
n/a	**Manually curated set**	**Literature**	**141**	**110**	**17**	**64**	**7**
HP:0000811	Abnormal external genitalia	HPO	1061	920	140	425	33
HP:0010461	Abnormality of the male genitalia	HPO	1053	907	142	424	34
HP:0010460	Abnormality of the female genitalia	HPO	512	447	72	223	15
HP:0000812	Abnormal internal genitalia	HPO	468	427	62	196	14
HP:0001827	Genital tract atresia	HPO	16	15	3	10	1
HP:0012244	Abnormal sex determination	HPO	20	17	2	8	1
HP:0003252	Anteriorly displaced genitalia	HPO	1	1	1	2	0
MP:0009198	abnormal male genitalia morphology	MP	1145	959	130	478	24
MP:0009208	abnormal female genitalia morphology	MP	696	587	89	304	18
MP:0002210	abnormal sex determination	MP	782	644	90	315	19
MP:0003936	abnormal reproductive system development	MP	99	91	12	46	1
			Grand total	**2284**	**313**	**1055**	**66**